MAIN, P., FISKE, S. J., HULL, S. E., LESSINGER, L., GERMAIN, G., DECLERCQ, J.-P. & WOOLFSON, M. M. (1982). *MULTAN*11/82. *A System of Computer Programs for the Automatic Solution of Crystal Structures from X-ray Diffraction Data*. Univs. of York, England, and Louvain, Belgium.
MIZUGUCHI, J. (1981). *Krist. Tech.* **16**, 695–700.
MIZUGUCHI, J. & WOODEN, G. (1991). *Ber. Bunsenges. Phys. Chem.* **95**, 1264.
PAULING, L. (1960). *The Nature of the Chemical Bond and the Structure of Molecules and Crystals*. Ithaca: Cornell Univ. Press.
ROCHAT, A. C., CASSAR, L. & IQUBAL, A. (1986). US Patent 4579949.

Acta Cryst. (1992). B**48**, 700–713

Nature of the Hydrogen Bond: Crystallographic *versus* Theoretical Description of the O—H···N(sp^2) Hydrogen Bond

BY ANTONIO L. LLAMAS-SAIZ AND CONCEPCION FOCES-FOCES*

UEI de Cristalografía, Instituto de Química-Física 'Rocasolano', CSIC Serrano 119, *E*-28006 *Madrid, Spain*

OTILIA MO AND MANUEL YAÑEZ*

Departamento de Química, Facultad de Ciencias, C-XIV, Universidad Autónoma de Madrid, Cantoblanco, E-28049 *Madrid, Spain*

AND JOSE ELGUERO

Instituto de Química Médica, CSIC, Juan de la Cierva 3, *E*-28006 *Madrid, Spain*

(*Received* 4 *January* 1991; *accepted* 9 *March* 1992)

Abstract

In order to analyze the characteristics of OH···N(sp^2) hydrogen bonds a survey of *R*—OH···N(sp^2) intermolecular interactions in organic crystals has been performed using the Cambridge Structural Database. Two subfiles of data, one containing 304 hydroxyl groups and the other 120 water molecules as donors, were selected and subjected to statistical analysis. In both sets the highest concentration of hydrogen-bond interactions occurs for almost linear arrangements. The strength of interactions involving *R*—OH groups depends on *R*, increasing as follows: C(sp^3) < N < C(sp^2). To complete this study we have carried out SCF calculations on 72 pyridine–water complexes at the 3-21G level. The nature of the hydrogen-bond interaction was also investigated by means of a topological analysis of both the charge density and the Laplacian of the charge density. This analysis revealed not only that charge-transfer interactions are sizeable but that they bear a direct relationship to the stability of the complex. Therefore, either the value of $\nabla^2\rho$ at the points of maximum charge concentration corresponding to the N(sp^2) lone pair, or the charge density at the hydrogen-bond critical point can be used as a suitable index for investigation of the relative stability of these hydrogen-bonded complexes. Our results show that there is fairly good agreement between the most outstanding features of the statistical survey and the SCF results.

Introduction

There is no need to stress the importance of the hydrogen bond in chemistry and in biology (Pimentel & McClellan, 1960; Schuster, Zundel & Sandorfy, 1976; Etter, 1990), and the increasing efforts towards a quantitative description of the hydrogen bond in LFER (linear free-energy relationships) (Taft, Abboud, Kamlet & Abraham, 1985). Nevertheless, different methods consider the hydrogen bond differently. Two of the more extreme pictures arise from classical crystallography (classical to differentiate it from electron density determinations) and from theoretical calculations. From a crystallographic point of view a hydrogen bond is a problem of the geometry of three particles *D*, H and *A* (*D*—H···*A*), namely the *D*—*A* distance and the angle at the hydrogen ($\angle DHA$). From these values, it is possible to conclude whether a hydrogen bond is present or not in a crystal and if it is strong or weak: a strong hydrogen bond is characterized by a short *D*—*A* distance and a $\angle DHA$ value near 180°. Although not categorically stated as such, this is the definition assumed by Taylor and Kennard (Taylor, 1981; Allen, Kennard & Taylor, 1983; Taylor, Kennard & Versichel, 1983,

* Authors for correspondence.

0108-7681/92/050700-14$06.00

1984; Taylor & Kennard, 1984) in all studies of hydrogen bonds using the Cambridge Structural Database (CSD) as well as by other authors (Kroon, Kanters, van Duijneveldt-van der Rijd, van Duijneveldt & Vliegenthart, 1975; Murray-Rust & Motherwell, 1979; Murray-Rust & Glusker, 1984; Görbitz, 1989; Llamas-Saiz & Foces-Foces, 1990; Jeffrey & Maluszynska, 1990).

Although theoretical calculations on hydrogen-bonded supersystems have geometrical implications (Kollman, 1977; Hehre, Radom, Schleyer & Pople, 1986), there are two fundamental effects of a hydrogen bond: (i) an energy stabilization over the separated molecules; (ii) the appearance of some electron density along the hydrogen bond.

Are these two pictures consistent? In order to answer this question, we decided to compare the distribution of geometries found in the CSD for the O—H···N(sp^2) hydrogen bond with calculations on the supersystem water···pyridine. Although strongly criticized by some authors (Bürgi & Dunitz, 1988; Krygowsky, 1990), most of them (Kroon, Kanters, van Duijneveldt-van der Rijdt, van Duijneveldt & Vliegenthart, 1975; Brown, 1976; Murray-Rust & Glusker, 1984; Gould, Gray, Taylor & Walkinshaw, 1985; Bartenev, Kameneva & Lipanov, 1987; Lesyng, Jeffrey & Maluszynska, 1988) consider that the experimental crystallographic populations correspond to a Boltzmann distribution, *i.e.* that if the number of examples is large enough, the scatter plot will resemble a probability distribution. The search of the CSD described more fully below has been restricted to *R*OH donors (*R* = H, C or N), excluding H_3O^+ and carboxylic acids in order to avoid cases of proton transfer to the basic nitrogen.

Theoretical calculations have been carried out on the simplest model, H_2O and pyridine. Pyridine is the smallest acceptor molecule which requires C_{2v} symmetry at the sp^2 nitrogen, so that only one octant (see Fig. 1) need be explored.

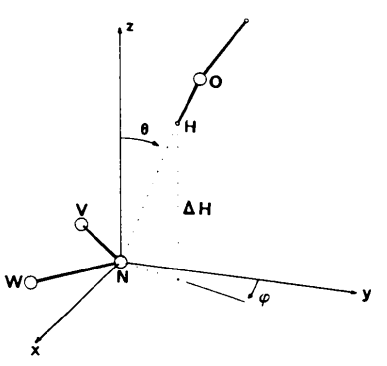

Fig. 1. The reference system. The N(sp^2) atom is chosen as the origin, the *y* axis as the line bisecting the *V*—N(sp^2)—*W* angle, the *z* axis perpendicular to the acceptor plane, and the *x* axis so as to define a right-handed system.

Statistical analysis of crystal structure data

Data retrieval

A survey of *R*—OH···N(sp^2) intermolecular interactions in organic crystals has been performed using the Cambridge Structural Database (January 1990 release with 78 641 entries) (Allen, Kennard & Taylor, 1983). Two subfiles of data were selected containing either hydroxyl groups or water molecules as donor and N(sp^2) as acceptors. Only data fulfilling the following conditions were included: (i) crystallographic *R* factor less than 0.10, (ii) data free of known crystallographic error at the 0.02 Å level, (iii) no disorder present, (iv) structures without metals, (v) experimentally determined H-atom positions, and (vi) diffractometric intensity data.

These subfiles were searched for hydrogen interactions with the conditions: O···N distances less than 3.1 Å (sum of van der Waals radii, with 1.52 Å for O and 1.58 Å for N) (Vainshtein, Fridkin & Indenbom, 1982), OH···N angle greater than 140°, and O—H and *R*—O—H distances and angles in the 0.70–1.15 Å and 85–135° ranges respectively. Thus, 304 and 120 hits were obtained for each respective subfile.

Statistical survey

The hydrogen interactions have been characterized by the usual parameters (O—H, O···N, H···N and O—H···N) (Taylor, Kennard, & Versichel, 1984), together with the displacements (ΔH) from the acceptor plane, and the spherical coordinates (θ, φ) of the H atom as defined in Fig. 1. Because of the symmetry of the acceptor, data in Tables 1, 2, 3 and 4 are referred to the $x, y, z > 0$ octant.

Table 1 presents selected geometrical parameters corresponding to O···N maximum distances of 3.1 and 2.9 Å, since just a few data (10 hits for each set) were found in the $3.0 < O\cdots N \leq 3.1$ Å range.

The normalized hydrogen positions, H′ (Taylor & Kennard, 1984), were computed using the mean O—H values observed by neutron diffraction in 62 and 29 structures (149 and 37 hits) containing *R*—OH groups and water molecules respectively. These two independent searches gave rise to unweighted mean O—H distances of 0.973 (28) and 0.960 (20) Å respectively (values in parentheses being the standard deviation of the sample). The corresponding values for the angle at the oxygen were 109.3 (30) and 107.0 (26)°.

The O···N and H···N histograms in Figs. 2(*a*,*b*) and 3(*a*,*b*) correspond closely to normal distributions, a conclusion based on inspection of normal probability plots (Abrahams & Keve, 1971). The distributions for the H_2O set are quite symmetrical and flat, as measured by the skewness ($g1$) and the kurtosis coefficients (−0.083, 2.706; −0.135, 2.701

Table 1. *Selected hydrogen-bonding geometries* (Å, °)

See Fig. 1 for the parameter definitions.

	R—O—H	O—H	O···N	H···N	O—H···N	ΔH	θ	φ
(*a*1) Donor *R*—OH, O···N ≤ 3.1 Å (304 CSD hits)								
Mean	107.5	0.91	2.806	1.93	163.7	0.36	79.1	10.4
Min.	86.2	0.70	2.552	1.47	140.6	0.00	39.8	0.0
Max.	134.2	1.15	3.077	2.43	179.8	1.59	90.0	37.6
(*a*2) Donor *R*—OH, O···N ≤ 2.9 Å (277 CSD hits)								
Mean	107.4	0.91	2.789	1.92	163.8	0.34	79.5	10.2
Min.	86.2	0.70	2.552	1.47	140.6	0.00	46.9	0.0
Max.	134.2	1.15	2.899	2.31	179.8	1.41	90.0	34.5
(*a*3) Donor *R*—OH, all data (304 CSD hits and normalized H positions)								
Mean	107.5	0.97	2.806	1.87	163.4	0.35	79.1	10.2
Min.	86.2	0.97	2.552	1.59	140.5	0.00	39.9	0.0
Max.	134.2	0.97	3.077	2.18	179.8	1.52	90.0	37.0
(*b*1) Donor H_2O, O···N ≤ 3.1 Å (120 CSD hits)								
Mean	107.1	0.90	2.889	2.02	166.1	0.45	76.9	8.3
Min.	92.3	0.70	2.703	1.73	141.5	0.00	24.8	0.0
Max.	125.4	1.15	3.046	2.30	179.6	2.01	90.0	24.1
(*b*2) Donor H_2O, O···N ≤ 2.9 Å (67 CSD hits)								
Mean	107.5	0.89	2.838	1.97	166.5	0.31	80.9	8.4
Min.	92.3	0.70	2.703	1.73	141.5	0.00	51.3	0.8
Max.	124.8	1.10	2.897	2.19	179.6	1.37	90.0	24.1
(*b*3) Donor H_2O, all data (120 CSD hits and normalized H positions)								
Mean	107.1	0.96	2.889	1.96	165.8	0.42	77.2	8.0
Min.	92.3	0.96	2.703	1.76	141.1	0.01	24.3	0.4
Max.	125.4	0.96	3.046	2.19	179.6	1.90	89.8	24.1

Table 2. *Distribution of θ and φ* (°)

θ range	φ range 0 < φ ≤ 10	10 < φ ≤ 20	20 < φ ≤ 30	30 < φ ≤ 40	40 < φ ≤ 50
(*a*) All intermolecular *R*—OH bonds (304 CSD hits)					
0.00 < θ ≤ 27.27	0	0	0	0	0
27.27 < θ ≤ 38.94	0	0	0	0	0
38.94 < θ ≤ 48.19	2	2	0	0	0
48.19 < θ ≤ 56.25	3	2	1	0	0
56.25 < θ ≤ 63.61	4	6	1	0	0
63.61 < θ ≤ 70.53	18	12	1	0	0
70.53 < θ ≤ 77.16	37	14	4	0	0
77.16 < θ ≤ 83.62	35	26	10	3	0
83.62 < θ ≤ 90.00	66	28	28	1	0
(*b*) *R*—OH, *R* = C(sp^3) (190 CSD hits)					
0.00 < θ ≤ 27.27	0	0	0	0	0
27.27 < θ ≤ 38.94	0	0	0	0	0
38.94 < θ ≤ 48.19	2	2	0	0	0
48.19 < θ ≤ 56.25	2	2	1	0	0
56.25 < θ ≤ 63.61	4	6	1	0	0
63.61 < θ ≤ 70.53	15	7	0	0	0
70.53 < θ ≤ 77.16	25	8	4	0	0
77.16 < θ ≤ 83.62	26	14	5	1	0
83.62 < θ ≤ 90.00	43	17	4	1	0
(*c*) *R*—OH, *R* = N (84 CSD hits)					
0.00 < θ ≤ 27.27	0	0	0	0	0
27.27 < θ ≤ 38.94	0	0	0	0	0
38.94 < θ ≤ 48.19	0	0	0	0	0
48.19 < θ ≤ 56.25	1	0	0	0	0
56.25 < θ ≤ 63.61	0	0	0	0	0
63.61 < θ ≤ 70.53	2	3	0	0	0
70.53 < θ ≤ 77.16	7	5	0	0	0
77.16 < θ ≤ 83.62	6	7	5	1	0
83.62 < θ ≤ 90.00	13	10	24	0	0
(*d*) All intermolecular H_2O bonds (120 CSD hits)					
0.00 < θ ≤ 27.27	0	0	1	0	0
27.27 < θ ≤ 38.94	0	1	0	0	0
38.94 < θ ≤ 48.19	3	0	0	0	0
48.19 < θ ≤ 56.25	2	3	0	0	0
56.25 < θ ≤ 63.61	3	2	0	0	0
63.61 < θ ≤ 70.53	7	4	2	0	0
70.53 < θ ≤ 77.16	10	4	0	0	0
77.16 < θ ≤ 83.62	26	8	3	0	0
83.62 < θ ≤ 90.00	27	13	1	0	0

Table 3. *Hydrogen-bonding geometries* (Å, °) *classified by the nature of the donor and acceptor groups together with the estimated mean values (i.e.* O···N*) and the standard deviation of the sample in parentheses*

No. of data		O···N	H···N	O—H···N
(*a*1) Donor, *R*—OH; acceptor, *V*—N(sp^2)—*W*				
	R			
1	O	2.725 (–)	1.75 (–)	166.5 (–)
84	N	2.794 (46)	1.92 (9)	166.2 (105)
29	C(sp^2)	2.762 (110)	1.90 (18)	161.9 (97)
190	C(sp^3)	2.819 (78)	1.95 (13)	165.0 (92)
(*a*2) Donor, C(sp^3)—OH; acceptor, *V*—N(sp^2)—*W*				
	V,*W*			
158	C,C	2.812 (74)	1.93 (12)	165.1 (89)
25	C,N	2.866 (93)	2.03 (17)	163.9 (111)
7	C,O	2.811 (58)	1.93 (8)	165.1 (88)
(*b*) Donor, H_2O; acceptor, *V*—N(sp^2)—*W*				
	V,*W*			
102	C,C	2.888 (69)	2.02 (11)	165.9 (88)
10	N,N	2.889 (96)	2.02 (19)	167.2 (97)
5	C,N	2.886 (77)	2.02 (11)	173.1 (20)
3	C,O	2.917 (99)	2.11 (17)	160.7 (120)

Table 4. *Hydrogen-bonding geometries* (Å, °) *for the structures containing pyridine as acceptor*

Ref.	*R*—O—H	O—H	O···N	H···N	O—H···N	ΔH	θ	φ
(*a*)	107.8	0.86	2.792	2.01	163.1	0.14	86.1	10.2
(*b*)	119.9	1.09	2.552	1.47	170.0	0.19	82.6	0.6
(*c*)	108.9	0.74	2.823	2.09	172.7	0.18	85.1	4.4

References: (*a*) Mootz & Wussow (1981); (*b*) Malarski, Majerz & Lis (1987); (*c*) Campsteyn, Dupont & Dideberg (1974).

versus 0 and 3 for a normal distribution) (Snedecor & Cochran, 1980). On the other hand, the *R*—OH distributions appear to be more unsymmetrical and sharper, showing *g*1 values up to 4.7 times the estimated standard error, σ ($\sigma^2 = 6$/No. of data) (0.659, 4.659; 0.421, 4.392 respectively).

For both cases the H′···N distributions are less symmetrical than the corresponding observed ones, as was previously found for the N—H···N(sp^2) interactions (0.496, 3.850; 0.382, 2.724 for the *R*—OH and H_2O sets respectively) (Llamas-Saiz & Foces-Foces, 1990).

Some differences were observed between the two groups of interactions (see Table 1). The O···N and H···N distances are significantly longer in the H_2O group at the 99.9% level (samples of unequal size) (Snedecor & Cochran, 1980); the linearity of the interactions, as measured by the O—H···N angle, is greater for this H_2O group, but at a 97.5% level. It should be noted that for 94 of the 120 water molecules the second H atom is also involved in O—H···N/O interactions. Figs. 2(*c*,*d*) and 3(*c*,*d*) show the corresponding histograms for the O—H···N angles before and after performing the conic corrections (Taylor & Kennard, 1984). 175 and 180° seem to be the most probable values for the *R*—OH and H_2O sets respectively. Within each group, no

differences were observed concerning the linearity of the interactions when analyzed *versus* the O···N distance, even when only the strongest ones were considered (O···N < 2.9 Å). Neither was any correlation observed when this angle was plotted *versus* either the θ or the φ angle (correlation values of −0.083, −0.279; −0.007, −0.039 for *R*—OH and H_2O). This lack of correlation was observed even when the analysis was carried out on θ, in small intervals of φ. Of the interactions shown in Table 1, 58.6% of the *R*OH bonds and 46.7% of the H_2O bonds show deviations, ΔH, from the acceptor plane which are smaller than the average for the strongest interactions. Table 2 and Fig. 4 (*DI*3000; Precision Visuals, 1987) show the (θ, φ) distributions after sorting the interactions into a trapezoidal grid of constant area. 33.2 and 44.2% of them involve an in-plane deviation (φ) of $\leq 10°$ and an out-of-plane deviation ($90 - \theta$) of less than 12.9° of the H atom from the lone-pair direction. The smaller percentage in the *R*—OH group could be due to the oxime structures (Tables 2*c* and 3). These oximes are part of an N—OH group of compounds, 50% of which show φ values > 15°, packed as dimers through the bonded N and O atoms; they show φ values clustered in the $20 < \varphi < 30°$ range (100.1° being the N—O—H angle).

Fig. 5 shows all fragments (the entire *R*—OH and H_2O sets) superimposed (Davenport & Hall, 1989). The greatest frequency corresponds to the theoretical lone-pair situation ($\theta = 90$ and $\varphi = 0°$).

If the nature of the atoms bonded to the donor atoms is taken into account, Table 3(*a*1), the strength of the interactions involving the *R*—OH group depends on *R*, increasing as follows: C(sp^3) < N < C(sp^2). The corresponding differences in the O···N distances appear to be significant at 99.9 and 80% levels respectively for the first and second inequality. (No bias was observed in the type of compounds involved in the last group.) If only the *R* = C(sp^3) case is considered, Table 3(*a*2), structures containing C atoms bonded to the N(sp^2) acceptor present stronger interactions (99.5% level) than when a C atom is replaced by a nitrogen.

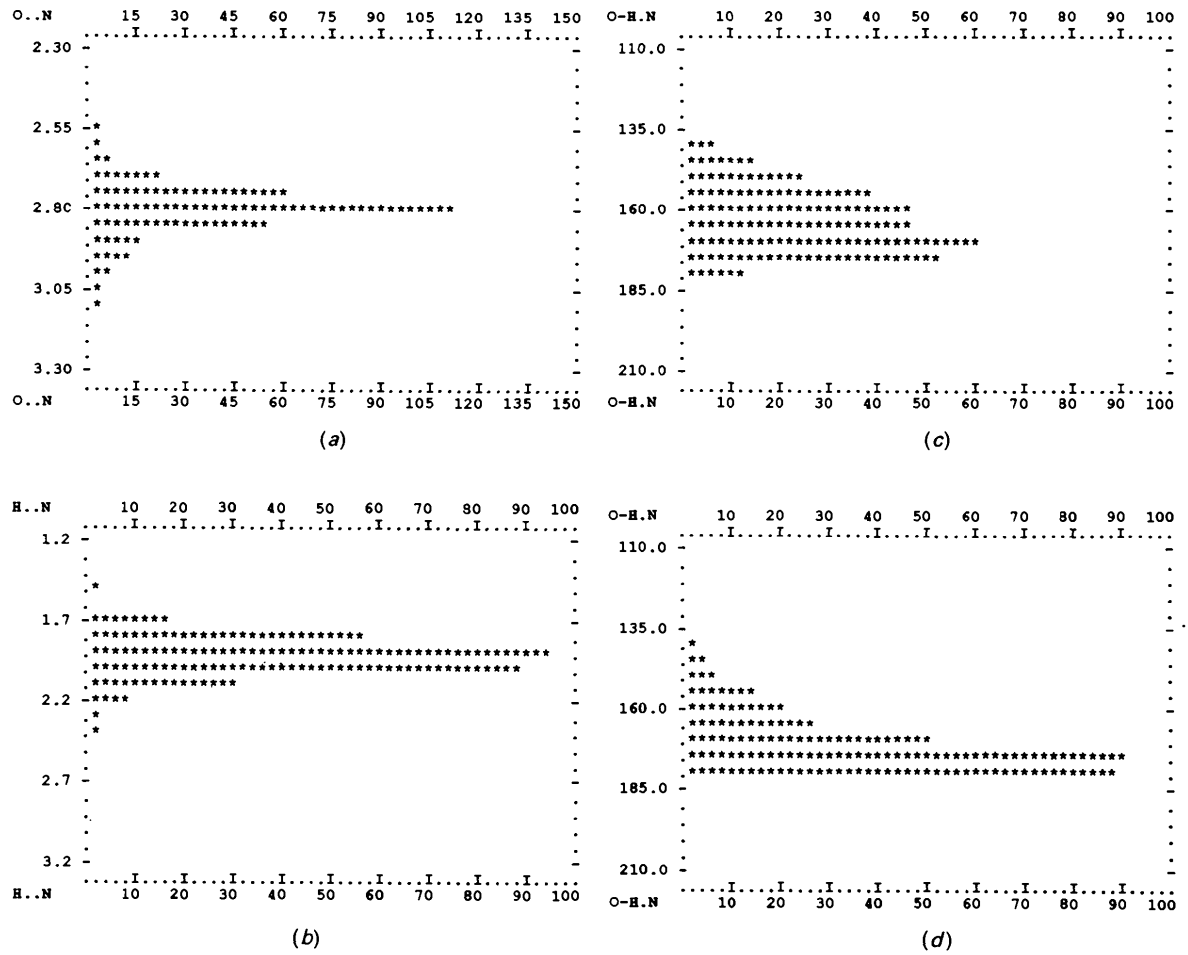

Fig. 2. Histograms for the *R*—OH donor group. (*a*) O···H, (*b*) H···N, (*c*) and (*d*) O—H···N before and after the conic correction.

No differences were observed for the H_2O set, Table 3 (*b*).

Finally, of all the structures considered in this study, only three contain pyridine as acceptor and H_2O, C(sp^2)—OH and C(sp^3)—OH as donors [pyridine trihydrate (Mootz & Wussow, 1981), 4-methylpyridine pentachlorophenol (Malarski, Majerz & Lis, 1987) and cortisol pyridine solvate (Campsteyn, Dupont & Dideberg, 1974)]. These show quite linear interactions, Table 4, and small deviations from the ideal N(sp^2) lone-pair direction. However, it is worth noting that the second of these displays the shortest O···N and H···N distances (Table 1). This may be due to the nature of the OH involved since the H···N distance is 0.43 Å shorter than the corresponding mean value in Table 1.

We conclude then, as pointed out in previous papers (Taylor, 1981; Taylor, Kennard & Versichel, 1984; Taylor & Kennard, 1984; Murray-Rust & Glusker, 1984; Görbitz, 1989; Llamas-Saiz & Foces-Foces, 1990) concerning hydrogen bonding in organic crystals, that the interactions appear to be quite linear. Some distortions were observed concerning direction when compared with that of the theoretical lone pair. In addition, some significant differences in the non-hydrogen distances are present, depending both on the nature of the donor and on the acceptor group. Moreover, both packing effects and the ability of the donor atom to take part in other interactions should not be neglected in such studies.

Computational details

The hydrogen-bond interactions between pyridine and water were investigated at the HF/3-21G level of theory. In order to be consistent with the statistical analysis of the previous section, these hydrogen interactions were geometrically characterized using the same parameters, *i.e.* θ and φ defined in Fig. 1. The values of θ and φ selected for our study are indicated in Tables 5–7. These values guarantee a practically homogenous distribution of points over the spherical surface which is defined for a given

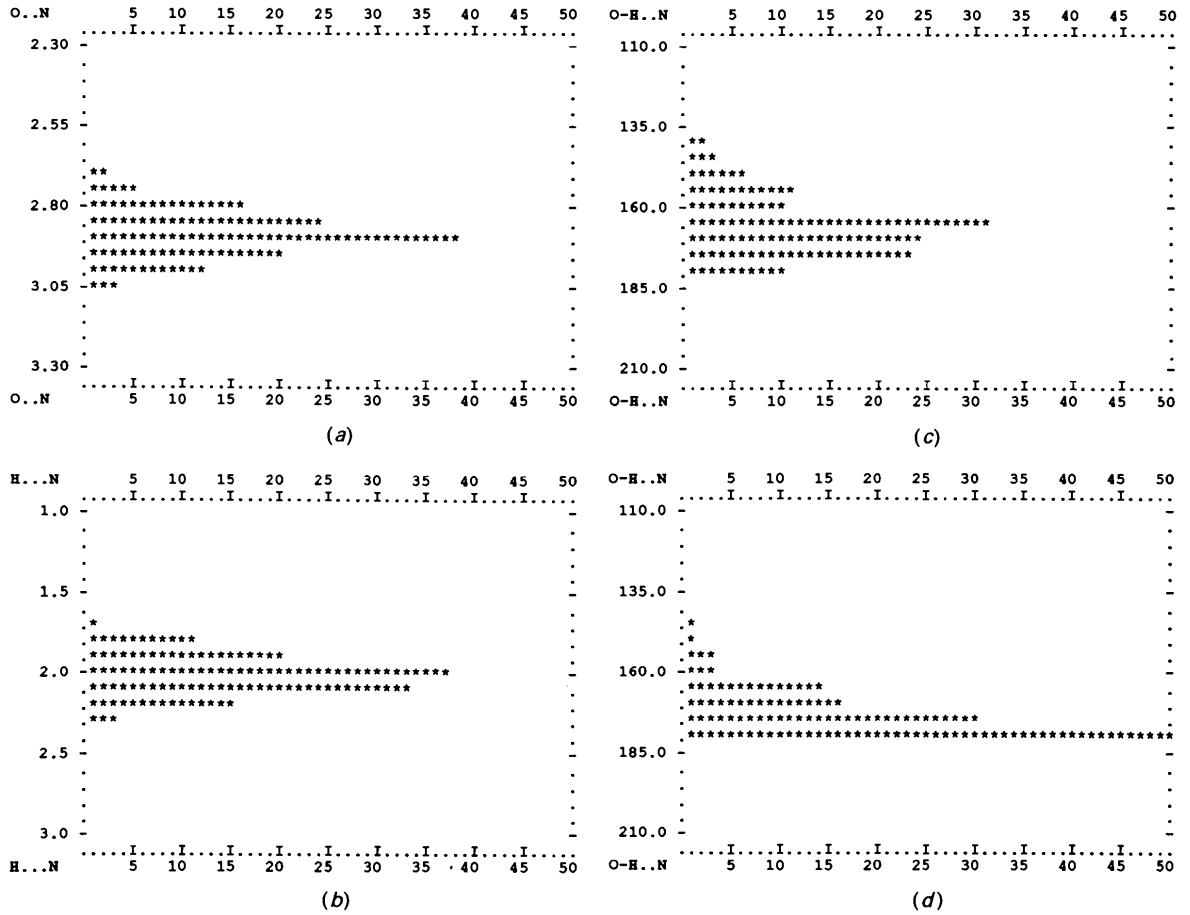

Fig. 3. Histograms for the H_2O donor group. (*a*)–(*d*) as in Fig. 2.

value of the N(pyridine)···H distance. Since our aim is to model the hydrogen-bond distribution in a quite rigid environment we have kept this distance constant at 1.86 Å, the value found for the first coordinated water molecule in pyridine trihydrate (Mootz & Wussow, 1981) after performing the H normalization (Taylor & Kennard, 1984).

To ensure the reliability of our SCF study it was necessary to eliminate any other arbitrariness from the model. Therefore, for each value of θ and φ we fully optimized the geometry of the complex without any further restriction. Consequently, a total of 72 systems were considered whose self-consistent-field dissociation energies, D_e, are defined as:

$$D_e = E_{SCF}(\text{pyridine}) + E_{SCF}(H_2O) - E_{SCF}(\text{complex}).$$

In general, an adequate description of hydrogen-bonded systems requires the inclusion of polarization functions in the basis set, but an optimization at the 6-31G* level of the 72 complexes considered in this study would be economically prohibitive. A reasonable compromise would be to evaluate the corresponding hydrogen-bond dissociation energies at the 6-31G*//3-21G level. However, to ensure reliability of this model it would also be necessary to check whether the relative stabilities of the complexes

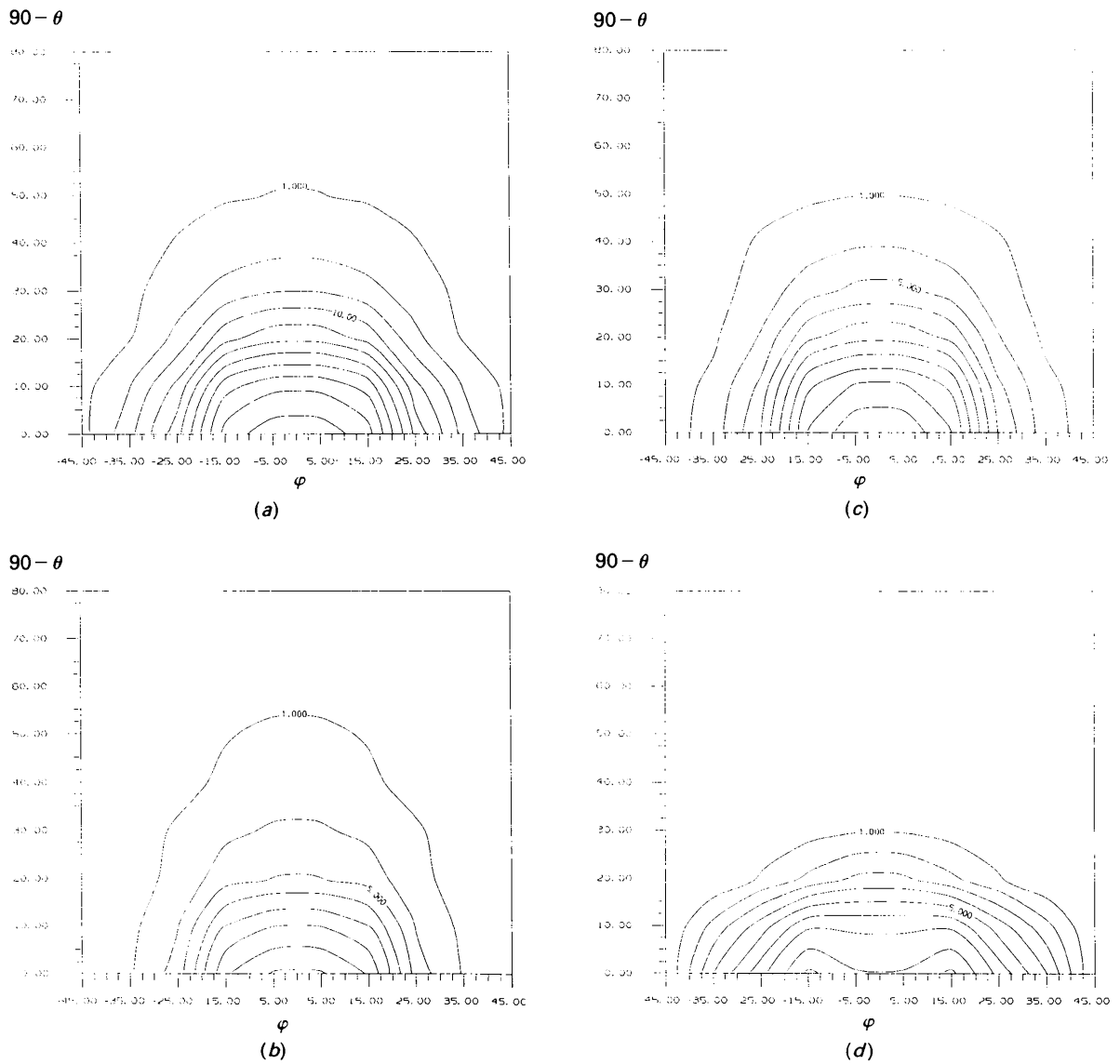

Fig. 4. The (θ, φ) distribution. The level curves have been drawn after performing an averaging between neighbouring values in order to smooth them. (*a*) *R*—OH, (*b*) H_2O, (*c*) C(sp^3)—OH and (*d*) N—OH donor groups.

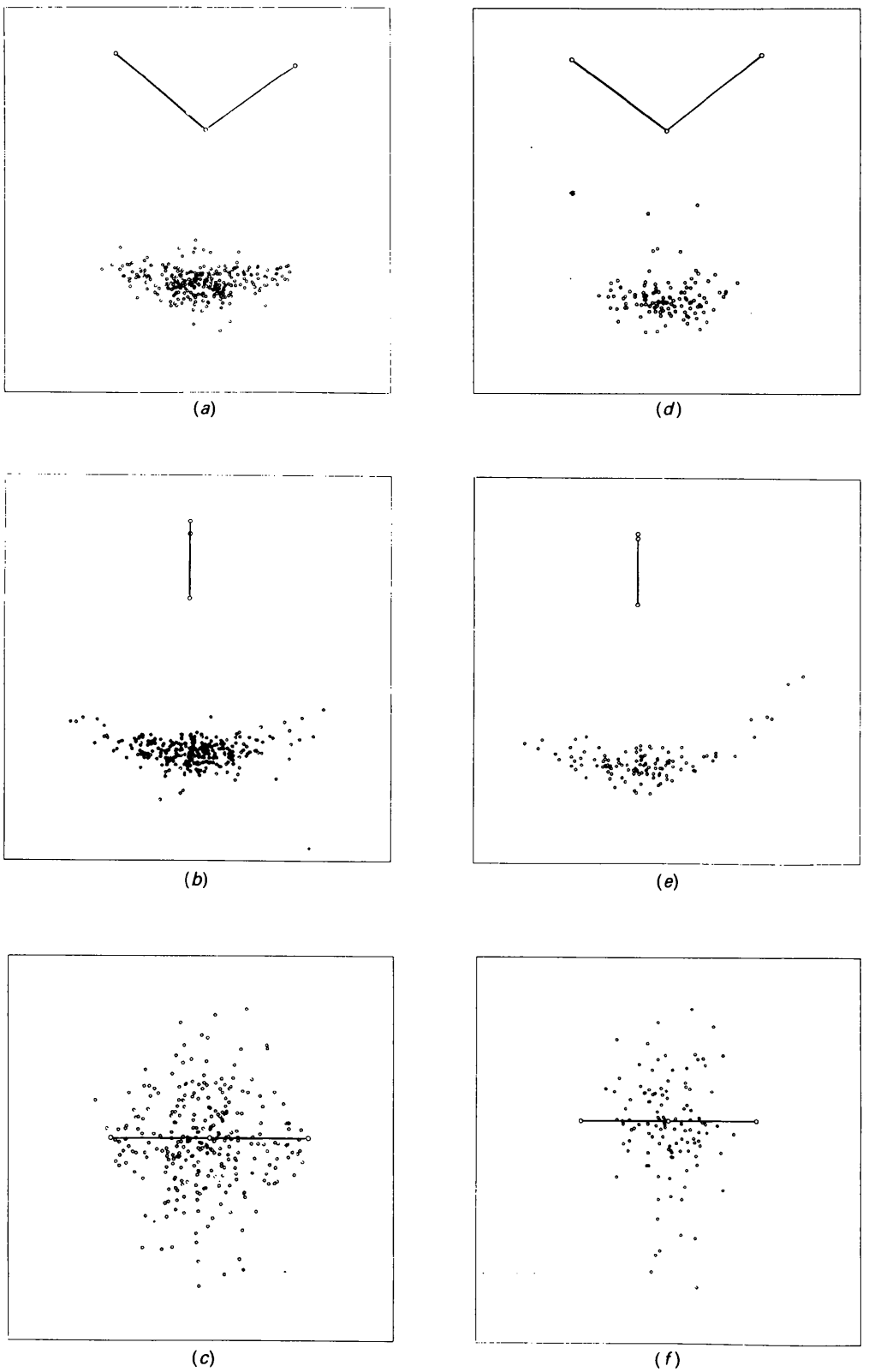

Fig. 5. The giant molecule (all fragments superimposed) projected along the z, x and y axes: (*a*), (*b*), (*c*) and (*d*), (*e*), (*f*) for the *R*—OH and H_2O sets respectively (see Fig. 1 for the reference system).

Table 5. *Dissociation energies, D_e (kcal mol^{-1}) of some pyridine–water hydrogen-bonded complexes*

ΔE (kcal mol^{-1}) are the relative stabilities of these complexes with respect to the global minimum ($\theta = 90.0$, $\varphi = 0°$). 1 kcal mol^{-1} = 4.1868 kJ mol^{-1}.

		D_e		ΔE	
		6-31G*//	6-31G*//	6-31G*//	6-31G*//
θ (°)	φ (°)	3-21G	6-31G*	3-21G	6-31G*
90.0	0.0	4.75	4.67	0.0	0.0
90.0	5.0	4.73	4.65	0.02	0.02
90.0	15.0	4.49	4.40	0.26	0.27
90.0	25.0	3.73	3.62	1.02	1.05
90.0	35.0	1.54	1.49	3.21	3.18
90.0	45.0	−3.83	−3.81	8.58	8.48

Table 6. *Relative stabilities ΔE (kcal mol^{-1}) of some pyridine–water hydrogen-bonded complexes with respect to the global minimum ($\theta = 90.0$, $\varphi = 0.0°$)*

1 kcal mol^{-1} = 4.1868 kJ mol^{-1}.

φ (°)	θ (°)	ΔE (6-31G*)	ΔE (3-21G)
0.0	90.0	0.0	0.0
0.0	56.891	1.38	1.83
0.0	46.427	2.21	2.90
0.0	30.059	3.87	4.94
0.0	22.919	4.75	5.95
0.0	3.174	7.77	9.29
5.0	90.0	0.02	0.01
5.0	46.427	2.25	2.94
15.0	90.0	0.25	0.24
15.0	56.891	1.70	2.16
15.0	46.427	2.54	3.24
25.0	90.0	1.01	0.71
25.0	46.427	3.10	3.90
35.0	90.0	3.21	2.02
35.0	3.174	7.99	9.57
45.0	90.0	8.58	6.38
45.0	76.365	7.53	6.42
45.0	2.919	6.73	7.98

obtained in 6-31G* single-point calculations at 3-21G optimized structures follow the same trend as those obtained using 6-31G* optimized geometries. To answer this question we reoptimized the structures of six of these complexes ($\theta = 90°$; $\varphi = 5$, 15, 25, 35 and 45°) and that of pyridine and water using a 6-31G* basis set. The corresponding dissociation energies are compared with those obtained at the 6-31G*//3-21G level in Table 5. Both the absolute dissociation energies, D_e, and the relative stabilities of the different complexes with respect to the global minimum ($\theta = 90°$, $\varphi = 0°$), ΔE, at the two levels of accuracy differ by less than 0.1 kcal mol^{-1}. This agreement is not surprising if one takes into account the fact that we are not interested in obtaining the global minimum of the pyridine–water complex (where basis-set effects may be crucial) but in the relative stabilities of complexes where *only* the orientation of the hydrogen-bond donor changes. Hence, to check the reliability of our conclusions based on 3-21G results it suffices to compare them with those obtained at the 6-31G*//3-21G level. To do so we have recalculated, at the latter level, the relative stabilities of 18 complexes (selected according to a *D*-optimal design) out of the 72 considered initially. As expected the absolute 6-31G*//3-21G

Table 7. *Calculated SCF 3-21G total energies, $-E$ (a.u.), hydrogen-bond dissociation energies, D_e (kcal mol^{-1}), O—H···N angles (°) and hydrogen-bond overlap populations as functions of the geometrical parameters θ and φ (°)*

1 kcal mol^{-1} = 4.1868 kJ mol^{-1}.

		$-E$	D_e	O—H···N	Overlap population
$\varphi = 0$	$\theta = 90.0$	320.91177	8.66	174.9	0.042
	80.404	320.91142	8.44	171.1	0.041
	76.365	320.91114	8.26	170.3	0.038
	67.081	320.91022	7.69	167.8	0.038
	56.891	320.90886	6.83	165.8	0.037
	46.427	320.90714	5.76	164.1	0.034
	37.772	320.90551	4.73	164.2	0.031
	30.059	320.90390	3.72	163.6	0.028
	22.919	320.90229	2.71	164.1	0.024
	16.143	320.90063	1.67	165.0	0.021
	9.596	320.89888	0.57	167.0	0.017
	3.174	320.89697	−0.63	169.9	0.013
$\varphi = 5$	$\theta = 90.0$	320.91175	8.65	174.0	0.042
	80.404	320.91136	8.40	172.5	0.041
	76.365	320.91109	8.23	170.1	0.041
	67.081	320.91016	7.65	169.4	0.040
	56.891	320.90880	6.80	166.0	0.037
	46.427	320.90708	5.72	164.1	0.034
	37.772	320.90545	4.69	165.3	0.031
	30.059	320.90385	3.69	163.8	0.028
	22.919	320.90192	2.48	165.4	0.024
	16.143	320.90060	1.65	165.2	0.021
	9.596	320.89886	0.55	166.9	0.017
	3.174	320.89696	−0.64	169.7	0.013
$\varphi = 15$	$\theta = 90.0$	320.91139	8.42	173.8	0.040
	80.404	320.91099	8.17	172.9	0.040
	76.365	320.91071	7.99	170.3	0.039
	67.081	320.90975	7.39	169.1	0.038
	56.891	320.90834	6.50	166.4	0.036
	46.427	320.90660	5.42	165.7	0.033
	37.772	320.90500	4.41	165.0	0.031
	30.059	320.90340	3.40	163.6	0.028
	22.919	320.90192	2.48	165.4	0.024
	16.143	320.90036	1.50	166.1	0.020
	9.596	320.89870	0.46	165.7	0.017
	3.174	320.89687	−0.69	170.2	0.013
$\varphi = 25$	$\theta = 90.0$	320.91064	7.95	173.9	0.037
	80.404	320.91204	7.70	171.2	0.038
	76.365	320.90990	7.48	171.3	0.039
	67.081	320.90880	6.80	171.9	0.036
	56.891	320.90730	5.84	169.5	0.033
	46.427	320.90556	4.76	168.7	0.031
	37.772	320.90405	3.81	167.9	0.029
	30.059	320.90265	2.93	167.6	0.026
	22.919	320.90128	2.08	167.4	0.023
	16.143	320.89990	1.21	167.9	0.020
	9.596	320.89840	0.27	168.9	0.016
	3.174	320.89672	−0.79	171.3	0.013
$\varphi = 35$	$\theta = 90.0$	320.90856	6.64	173.4	0.037
	76.365	320.90777	6.15	174.1	0.035
	56.891	320.90525	4.57	174.6	0.033
	46.427	320.90373	3.62	174.0	0.029
	37.772	320.90251	2.85	172.2	0.026
	30.059	320.90141	2.15	171.0	0.024
	22.919	320.90034	1.47	170.1	0.021
	16.143	320.89923	0.79	170.0	0.019
	9.596	320.89795	0.01	170.4	0.017
	3.174	320.89652	−0.91	172.8	0.013
$\varphi = 45$	$\theta = 90.0$	320.90164	2.28	173.7	0.036
	76.365	320.90153	2.24	176.8	0.033
	56.891	320.90102	1.91	178.6	0.030
	46.427	320.90061	1.65	179.9	0.027
	37.772	320.90017	1.38	177.6	0.024
	30.059	320.89967	1.07	175.3	0.022
	22.919	320.89909	0.68	174.1	0.020
	16.143	320.89839	0.26	172.7	0.017
	9.596	320.89750	−0.29	172.8	0.015
$\varphi = 55$	$\theta = 76.365$	320.88635	−7.29	176.2	0.031
	56.891	320.89227	−3.58	179.4	0.027
	46.427	320.89515	−1.77	179.4	0.023
	30.059	320.89731	−0.41	179.4	0.020
	22.919	320.89751	−0.29	177.0	0.018

hydrogen-bond dissociation energies (see Table 5) are smaller than the 3-21G values reported in Table 7. However, changes in relative stabilities (see Table 6) are much smaller and most importantly, a fairly good correlation exists between both sets of values, which obeys the equation:

$$\Delta E(\text{6-31G*//3-21G}) = 3.149 + 1.086\Delta E(\text{3-21G}) - 3.243\cos^2\varphi - 6.232\cos^2(90-\theta) + 4.207\cos^2\varphi\cos^2(90-\theta); \quad r^2 = 0.997. \quad (1)$$

In order to analyze the nature and variation of the interactions for the different geometrical arrangements of the hydrogen-bond donor with respect to the acceptor we have evaluated the Laplacian of the charge density for some specific systems. As shown by Bader (Bader & Essen, 1984; Bader, MacDougall & Lau, 1984; Wiberg, Bader & Lau, 1987), $\nabla^2\rho$ identifies regions of space wherein the electronic charge of a given system is locally concentrated or depleted. In the first situation $\nabla^2\rho(r) < 0$, whereas in the latter $\nabla^2\rho(r) > 0$. In general, negative values of $\nabla^2\rho$ are typical of covalent bonds, where charge is concentrated in the interatomic region leading to an energy lowering associated with the predominance in this region of the potential-energy density. By contrast, positive values of $\nabla^2\rho$ are associated with interactions between closed-shell systems, as in typical ionic bonds, hydrogen bonds or van der Waals molecules, where electronic charge is depleted in the interatomic region, leading to a predominance of the kinetic energy density.

We have also located the bond critical points of the N···H hydrogen bond for some specific cases. At the bond critical points the electronic charge density, ρ, has one positive curvature (λ_3) and two negative curvatures (λ_1, λ_2), *i.e.* it is a minimum along the bond axis and a maximum along any other direction, and can therefore be unequivocally located. Since the nature of the atoms involved in the hydrogen bond does not change, the bond characteristics (ρ and $\nabla^2\rho$) evaluated at the bond critical points should offer quantitative information on the variation of the strength of the hydrogen-bond linkage when the relative orientation of the hydrogen-bond donor changes.

A topological analysis of the Laplacian of the charge density can also contribute to our understanding of the role played by the acceptor lone pair. Actually, the points of the maximum charge concentration correspond to the attached lone pairs and they can easily be located by searching for the critical points (maxima) of the Laplacian of the charge density. We aim to show that there is a clear relationship between the value of $\nabla^2\rho$ at the donor lone pair and the dissociation energy (D_e) of the hydrogen-bonded complex.

We have also checked whether the conclusions based in this topological analysis are basis-set dependent by comparing the results obtained, for some suitable examples, at the 3-21G//3-21G and 6-31G*//3-21G levels of theory, respectively.

Comparison of theory and experiment, and characteristics of the O—H···N(sp^2) hydrogen bond

3-21G total energies of the complexes studied and their hydrogen-bond dissociation energies are summarized in Table 7. Although a detailed discussion of the structure of these complexes (which is available from the authors upon request†) is not the aim of our study, the O—H···N angles, which measure the linearity of the hydrogen bond and are significant geometrical parameters, have also been included in the table. Table 7 also summarizes the overlap population between the pyridine nitrogen and the water proton, since as we shall show later, it is relevant for the discussion of the relative stability of the different complexes.

In this respect it is helpful to consider Fig. 6 which shows a two-dimensional plot of the hydrogen-bond dissociation energies as a function of the geometrical parameters θ and φ. It can easily be found, by means of equation (1) of the previous section, that this representation does not change significantly when the 6-31G*//3-21G values are used. It is obvious from both Table 7 and Fig. 6 that the predicted (θ, φ) distribution is not random, in agreement with the statistical analysis of the previous section and with the conclusions of Llamas-Saiz & Foces-Foces (1990), and in contrast with those of Murray-Rust & Glusker (1984). Our results show that hydrogen bonds are particularly stable for low values of φ and values of θ close to 90°. However, the agreement with the statistical survey carried out above is even more quantitative if one takes into account the fact that the most stable complex corresponds to $\theta = 90$ and $\varphi = 0°$ but that the system is destabilized by only 0.4 kcal mol^{-1} when the hydrogen bonds are 13.6° out of the acceptor plane and by 0.3 kcal mol^{-1} when they are about 15° away from the line which bisects the C—N—C angle. Of course Fig. 6 cannot be compared directly with Fig. 4, since the former is an energy distribution rather than a probability distribution. Nevertheless, assuming a Boltzmann distribution we can reasonably suppose that, at room temperature, all structures which lie within 1 kcal mol^{-1} from the optimum structure (Kroon,

† In addition, a list of CSD refcodes and references has been deposited with the British Library Document Supply Centre as Supplementary Publication No. SUP 55110 (48 pp.). Copies may be obtained through The Technical Editor, International Union of Crystallography, 5 Abbey Square, Chester CH1 2HU, England, or direct from the authors.

Kanters, van Duijneveldt-van der Rijdt, van Duijneveldt & Vliegenthart, 1975) are very likely to occur. From the results of Table 5 this would correspond to values of $\theta > 67°$ and values of $\varphi < 30°$, and according to the statistical survey of the previous section, 93% of the experimental structures investigated are within this range. It can be seen, however, that a few experimental structures correspond to values of θ and φ which are clearly beyond this range. If we assume as reasonable the 1 kcal mol^{-1} energy gap with respect to the global mimimum and take into account the relative dissociation energies of Table 5, these structures would correspond to crystals with an effective temperature of 800–1000 K.

Table 7 also shows that the hydrogen-bond dissociation energies rapidly decrease as θ goes beyond 60°. Actually, for values of θ close to zero (θ = 3.174°) the complex is less stable than the separated subunits. Of course this is a consequence of the fact that we kept the N···H distance frozen, but it clearly illustrates that for these relative orientations of the hydrogen-bond donor the stability of the complex is quite low. Similarly, when φ increases the complex becomes less and less stable. However, the variation is not gradual. It may be observed that the stability of the complex decreases quite slowly for values of φ smaller than 25°. For 35° the destabilization is more significant and for $\varphi = 45°$ can be considered dramatic.

Let us look closer at the stability variation of these complexes and to do so let us first focus our attention on the case where $\varphi = 0°$. It is obvious that, as indicated above, the most stable structure corresponds to $\theta = 90°$ which has a dissociation energy of 8.66 kcal mol^{-1}. When θ decreases, *i.e.* when the angle out of the molecular plane ($90 - \theta$) increases, the complex becomes less and less stable, but more importantly the stability decreases roughly as $\cos(90 - \theta)$. This seems to indicate, in agreement with other analyses in the literature (Hurst, Fowler, Stone & Buckingham, 1986), that one important contributor to the stability of the complex would be the electrostatic interactions, especially those between the charge on the proton of the donor and the dipole moment of the acceptor. However, it must be emphasized that purely electrostatic calculations are unable to reproduce the experimental geometries of van der Waals complexes (Baiocchi, Reiher & Klemperer, 1983). The formation of the van der Waals complex produces a distortion of the charge distribution which is apparent in the characteristics of the bond critical points for the corresponding hydrogen bonds. As illustrated in Table 8, as θ increases the charge density at the bond critical point (at both levels of accuracy) also increases showing that a more effective charge-dipole interaction results in a large charge transfer from the acceptor into the hydrogen-bond region and therefore in a greater stability of the corresponding hydrogen-bonded complex. The situation is apparently different when considering the variation of φ, since as indicated above, the stability of the complex decreases dramatically for values of $\varphi > 45°$. However this can easily be explained. Let us consider for the sake of simplicity the case of $\theta = 90°$. As before, the most stable situation corresponds to $\varphi = 0°$ and the stability of the complex decreases as φ increases, *i.e.* as the hydrogen bond moves away from the axis of the nitrogen lone pair. For values of $\theta < 45°$ the stability of the complex decreases roughly as $\cos\varphi$. This is consistent with the isotropic nature of the charge distribution of the pyridine nitrogen lone pair: it is practically identical in the plane of the molecule and in the plane perpendicular to it which bisects the C—N—C angle (see Fig. 7). In other words, from the topological characteristics of the nitrogen lone pair one should expect roughly the same behavior of the complex stability upon θ or φ variations and this is indeed the case for values of $\varphi < 35°$. When φ goes beyond this value a strong repulsion between the proton of the hydrogen-bond donor and the C—H proton in the α position with respect to the pyridine nitrogen appears. This repulsion begins to be dramatic for $\theta = 45°$ and for $\varphi = 55°$ is so large that the complex is less stable than the separated subunits (see Table 7). In this respect, it must also be noted that these repulsive interactions are somewhat underestimated at the 3-21G level with respect to the 6.31G* level. Accordingly, the instability of the complex becomes important at lower values of φ when the latter basis set is used. This picture is consistent

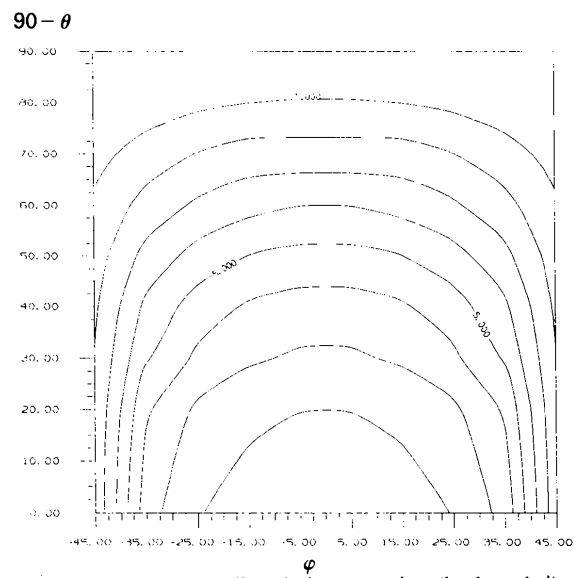

Fig. 6. Hydrogen-bond dissociation energies (kcal mol^{-1}) of pyridine–water complexes as a function of the geometrical parameters θ and φ (°).

Table 8. *Bond critical point properties of the hydrogen bonds of some pyridine–water complexes*

ρ is in e Å^{-3}, $\nabla^2\rho$ and λ in e Å^{-5}, R in Å, and φ and θ in °. Columns marked *a* correspond to 3-21G//3-21G results, those marked *b* correspond to 6-31G*//3-21G values.

		ρ		$\nabla^2\rho$		λ_1		λ_2		λ_3		R	
		a	*b*	*a*	*b*	*a*	*b*	*a*	*b*	*a*	*b*	*a*	*b*
$\varphi = 0$	$\theta = 90.0$	0.270	0.243	2.554	2.699	−1.518	−1.349	−1.494	−1.301	5.567	5.350	1.22	1.23
$\varphi = 0$	$\theta = 44.427$	0.256	0.229	2.651	2.735	−1.373	−1.229	−1.325	−1.157	5.350	5.121	1.21	1.22
$\varphi = 0$	$\theta = 22.919$	0.236	0.216	2.699	2.771	−1.205	−1.084	−1.181	−1.036	5.085	4.891	1.20	1.21
$\varphi = 0$	$\theta = 3.174$	0.229	0.209	2.771	2.795	−1.084	−0.964	−1.036	−0.940	4.892	4.700	1.19	1.20
$\theta = 90.0$	$\varphi = 5.0$	0.270	0.243	2.554	2.747	−1.518	−1.325	−1.494	−1.277	5.567	5.350	1.22	1.24
$\theta = 90.0$	$\varphi = 25.0$	0.263	0.236	2.602	2.747	−1.494	−1.253	−1.470	−1.229	5.542	5.230	1.23	1.23
$\theta = 90.0$	$\varphi = 35.0$	0.256	0.223	2.651	2.795	−1.446	−1.157	−1.422	−1.157	5.518	5.109	1.22	1.22

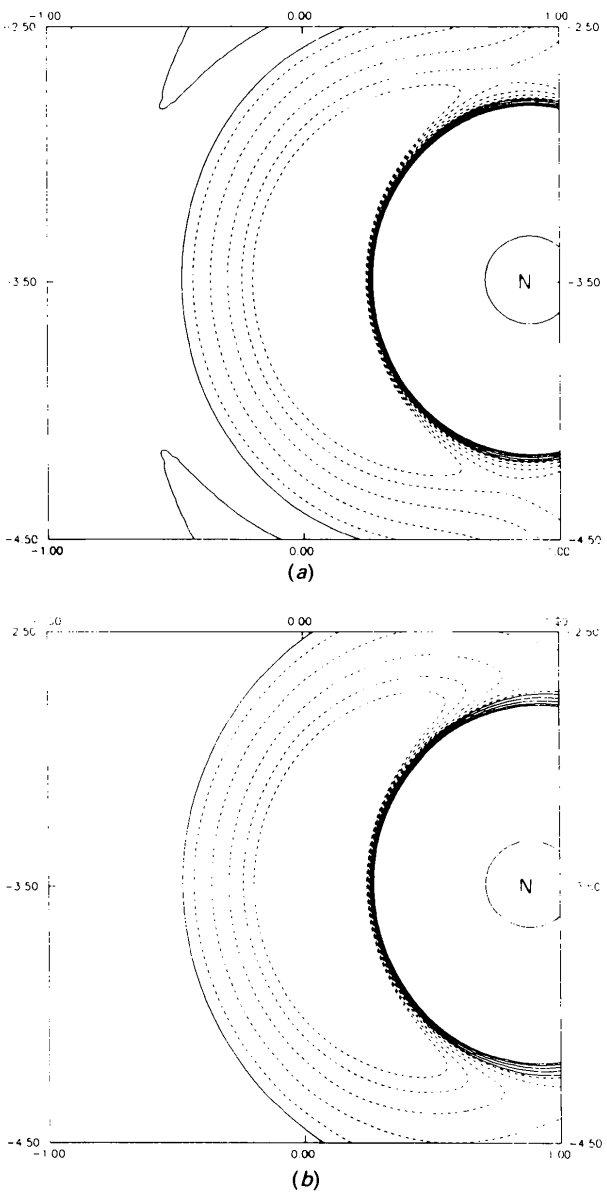

(*a*)

(*b*)

Fig. 7. Laplacian of the charge density of the nitrogen lone-pair region of pyridine: (*a*) molecular plane, (*b*) symmetry plane perpendicular to the plane of the molecule. Dashed lines correspond to $\nabla^2\rho < 0$, continuous lines correspond to $\nabla^2\rho > 0$.

with the fact that for $\varphi > 45°$ the stability of the complex increases as θ decreases in contrast to the behavior for $\varphi < 45°$. Obviously, in the former cases a decrease in the value of θ implies a considerable attenuation of this repulsion since the distance between the C—H proton and the water proton decreases noticeably. Furthermore, there is fairly good agreement between these limiting values of θ and φ and those found from the statistical analysis of the previous section which shows that while the maximum and minimum values of θ in the crystal structures are about 90 and 25° respectively, those for φ cover a much smaller range: 0 to 24°. Similar results were reported previously (Llamas-Saiz & Foces-Foces, 1990) for N—H···N(sp^2) hydrogen bonds.

The lone pair of the hydrogen-boind acceptor is directly involved in the charge transfer which takes place within the bonding region as revealed by a topological analysis of the Laplacian of the charge density. At the level of accuracy considered in this work, the Laplacian of the charge density of the hydrogen-bond acceptor (pyridine) shows a maximum (in absolute value) at 0.384 Å from the nitrogen nucleus, which corresponds to the maximum concentration of charge of the nitrogen lone pair. The value of the charge density at this point is 4.238 e Å^{-3}. Table 9 shows that when the pyridine–water complex is formed, the value of $\nabla^2\rho$ increases while that of ρ decreases, showing that the charge accumulated at the hydrogen-bonded region essentially comes from the pyridine nitrogen lone pair. Furthermore, the increase in the value of $\nabla^2\rho$ is greater the greater the stability of the complex and the maximum of the charge concentration moves away from the nitrogen. Simultaneously, the OH bond directly involved in the hydrogen bond lengthens. Four features are important from the results of Table 9: (i) In agreement with our previous discussion, the charge-density lowering at the pyridine lone pair is similar for θ and φ variations, provided $\varphi <$ 25 and $\theta > 65°$. In other words, the lone pair behaves, within this range, as a quite isotropic charge distribution. (ii) The maxima of the $\nabla^2\rho$ can be considered as suitable indices for measuring the

Table 9. *Charge density* ρ (e Å^{-3}) *and Laplacian of the charge density* $\nabla^2\rho$ (e Å^{-5}) *at the points of maximum charge concentration corresponding to the nitrogen lone pair of some pyridine–water hydrogen-bonded complexes*

Columns marked *a* correspond to 3-21G//3-21G results, those marked *b* correspond to 6-31G*//3-21G values. R_{LP} represents the distance (Å) from these points to the nitrogen nucleus (the corresponding 3-21G values for the isolated pyridine are: $\rho = 4.238$, $\nabla^2\rho = -73.499$, $R_{LP} = 0.384$). R(O—H) is the length (Å) of the O—H bond involved in the hydrogen bond. φ and θ are in °.

		ρ		$\nabla^2\rho$		R_{LP}		R(O—H)
		a	*b*	*a*	*b*	*a*	*b*	*a*
$\varphi = 0$	$\theta = 90.0$	4.089	4.056	−66.993	−82.438	0.387	0.387	0.979
$\varphi = 0$	$\theta = 44.422$	4.130	4.065	−68.679	−83.179	0.386	0.387	0.975
$\varphi = 0$	$\theta = 22.919$	4.157	4.069	−70.125	−83.680	0.386	0.386	0.972
$\varphi = 0$	$\theta = 3.174$	4.191	4.075	−71.330	−84.083	0.385	0.386	0.969
$\theta = 90.0$	$\varphi = 5.0$	4.103	4.059	−67.475	−82.791	0.386	0.385	0.978
$\theta = 90.0$	$\varphi = 25.0$	4.116	4.062	−68.198	−83.009	0.386	0.386	0.974
$\theta = 90.0$	$\varphi = 35.0$	4.123	4.065	−68.679	−83.187	0.385	0.386	0.972

stability of hydrogen-bonded complexes. (iii) The geometry reorganization of the hydrogen-bond donor, although small, is not negligible (Liu & Dykstra, 1986; Bulanin, Bulychev & Tokhadze, 1989). This geometry distortion bears a clear relationship to the stability of the complex and to the charge redistribution of the hydrogen-bond acceptor. A small geometry distortion of the latter, essentially affecting the CNC endocyclic angle, is also observed. (iv) Although the absolute value of the Laplacian changes appreciably on going from the 3-21G to the 6-31G* basis set both sets of values follow a similar trend; on the other hand the calculated non-bonded charge densities and their relative positions are not very sensitive to the basis set used.

According to our previous discussion, it seems evident that a clear relationship exists between the angular distribution of the hydrogen bonds and the stability of the complex, due to a more effective electrostatic interaction, as a primary mechanism, which leads to a more effective charge transfer from the acceptor into the hydrogen-bond region. Should this picture be correct, some relationship would exist between the stability of the hydrogen bond and the charge accumulated at the bond critical point or alternatively, between the hydrogen-bond stability and its overlap population. Both correlations exist and as a suitable illustration we have chosen that involving the latter (see Fig. 8). It is evident from Fig. 8 that quite a good linear correlation exists between the stability of the hydrogen-bond complexes and the charge accumulated in the hydrogen-bond region explaining why the angular distribution of the hydrogen bonds is not random. It should also be noted that complexes with $\varphi > 45°$ do not follow this linear relationship for the reasons mentioned above.

Slightly non-linear hydrogen bonds have often been reported in the literature (Del Bene, 1983; Frisch, Pople & Del Bene, 1985; Somasundram, Amos & Handy, 1986; Sadlej & Roos, 1989). In our modeling of pyridine–water complexes we have also found that for all values of θ and φ investigated the hydrogen bonds deviate slightly from linearity. This deviation is small for the most stable configurations. The O—H···N angle is about 175° for the global minimum which agrees nicely with the most probable value from our statistical survey. When the proton donor moves away from the pyridine plane the linearity of the hydrogen bond decreases, but it remains practically constant and equal to 165° for a wide range of values of θ ($20 \le \theta \le 60°$). It is interesting to note that the experimental results indicate that the average value of this angle is about 164–166°. Of course, in this respect, the comparison between theoretical and experimental results cannot be carried too far, because in the crystal there are secondary interactions which cannot be taken into account in our modeling. However, we may assume that the observed deviations from linearity may bear some relationship to the relative orientation (θ, φ) of the donor.

Our model also shows that for these particular complexes the linearity of the hydrogen bond is

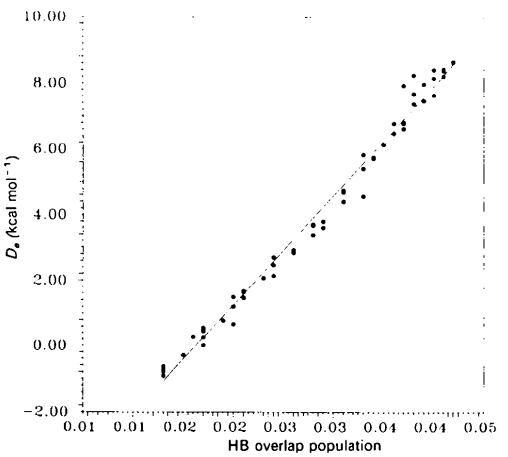

Fig. 8. Linear correlation between the hydrogen-bond dissociation energies of pyridine–water complexes and the overlap population of the corresponding hydrogen bond.

much more sensitive to θ than to φ variations. Actually, when φ goes from 0 to 45° the O—H···N angle changes from 174.9 to 173.7°, while for changes in θ from 90 to 60° it changes to 165.8°. This may be easily understood in the light of differences in the electronic distribution of the pyridine in the plane of the molecule and in the symmetry plane perpendicular to it. In fact, when the hydrogen-bond donor moves out of the pyridine plane a secondary interaction between the second water proton and the charge density concentrated above (and below) the pyridine plane appears (see Fig. 9). This attractive interaction forces a bending movement of the hydrogen-bond donor which results in a 10° decrease in the linearity of the bond. By contract, when φ varies this interaction does not change and the linearity of the hydrogen bond is not affected. Only for values of φ greater than 35° and for small deviations from the molecular plane (θ close to 90°) are the hydrogen bonds close to linear due to strong repulsion by the C—H proton. It must be pointed out, however, that this analysis cannot be applied directly to the situation in the crystal, since in a rigid medium movement of the hydrogen-bond donor is strongly hindered.

Concluding remarks

The polar-cap electron density loses its radial symmetry when hydrogen bonded. At this moment, the in-plane situation ($\theta = 90°$) and the out-of-plane situation become quite different, the first is sensitive to steric effects (pyridine α-hydrogens) whereas the second experiences the hydrogen-bond attraction of the π-bonding basicity (Legon & Millen, 1987).

Pure electrostatic models of hydrogen bonds need to be highly elaborated, up to octapoles, to describe the geometry of van der Waals complexes (Buckingham & Fowler, 1983) or the vibrational transition frequency shifts due to hydrogen bonds (Liu & Dykstra, 1986). Nevertheless, the general opinion is that although electrostatic interactions are of paramount importance (Mitchell & Price, 1989, 1990) other terms such as polarization of charge, dispersion, charge transfer and exchange effects play an important role (Liu & Dykstra, 1986; Reed, Weinhold, Curtiss & Pochatko, 1986), to the point that some authors (Vedani & Dunitz, 1985) have pointed out that the importance of electrostatic contributions to force-field models had probably been overestimated. Our topological analysis of both the charge density and the Laplacian of the charge density reveal that charge-transfer interactions are not only sizeable but bear a direct relationship to the stability of the complex. In fact, a crude electrostatic approach could not be enough to describe these complexes since both charge redistribution of the interacting subunits and geometry distortions are non-negligible. Our topological approach offers a way of evaluating quantitatively the charge-transfer interactions and therefore determining, at least in relative terms, the stability of the complex. It also seems to confirm that the angular distribution of the hydrogen bond is basically governed by the intrinsic characteristics of the charge density of the acceptor lone pair. However, there are situations in which, as mentioned above, steric effects are also important.

In general there is remarkably good agreement between the most outstanding features of our statistical survey of experimental data and the theoretical results obtained from our SCF modeling of the pyridine–water complexes. This agreement may be summarized by stating that the angular distribution

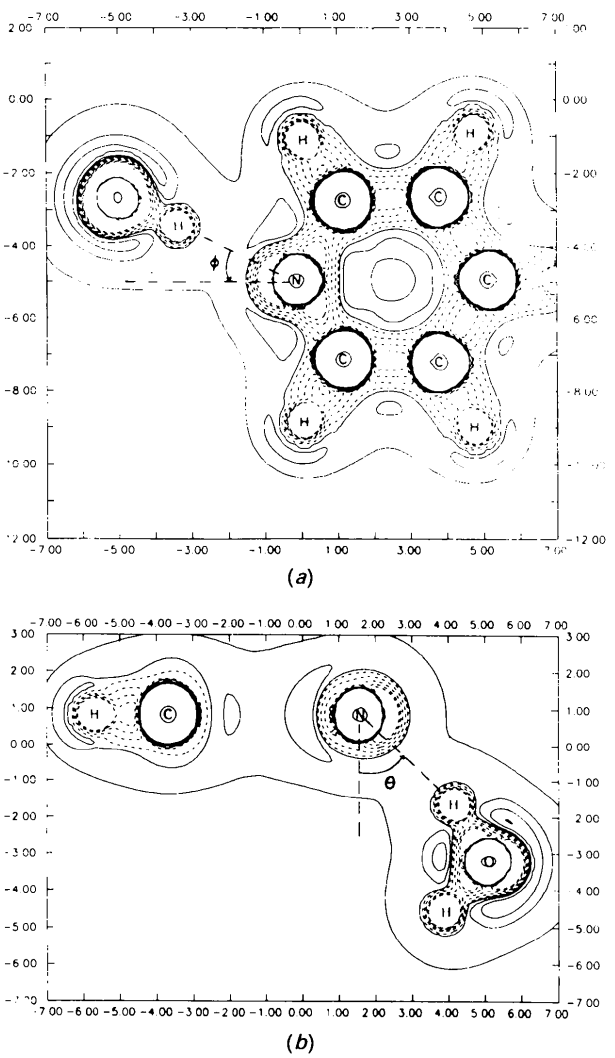

Fig. 9. Laplacian of the charge density of the pyridine–water complex corresponding to: (*a*) $\varphi = 25$, $\theta = 90°$; (*b*) $\varphi = 0$, $\theta = 44.422°$. Same conventions as in Fig. 7.

corresponds essentially to the dissociation energies distribution assuming a Boltzman-type weighting.

Situations exist in crystals which correspond geometrically to a hydrogen bond but which the theory does not support, *i.e.* positions of the H atom with values of $\theta \leq 60°$ and/or $\varphi \geq 30°$. These would correspond to crystals with a quite high (~ 1000 K) effective temperature. The existence of these structures in the crystal clearly indicates that other interactions besides those of the hydrogen bond considered may be quite stabilizing.

We thank Mr S. García Asensio for assistance with the *DI*3000 package, and the Dirección General de Investigación Científica y Técnica for financial support (PB87-0291 and PB87-0131).

Most of the calculations for the statistical study were carried out using the CSD and a VAX 6410 computer. SCF calculations were either carried out at the CC/UAM Computational Center or on an RISC/6000 computer. We also thank the CICYT of Spain for a generous allocation of computing time on the CRAY computer at CASA.

References

ABRAHAMS, S. C. & KEVE, E. T. (1971). *Acta Cryst.* A**27**, 157–165.

ALLEN, F. H., KENNARD, O. & TAYLOR, R. (1983). *Acc. Chem. Res.* **16**, 146–153.

BADER, R. F. W. & ESSEN, H. (1984). *J. Chem. Phys.* **80**, 1943–1960.

BADER, R. F. W., MACDOUGALL, P. J. & LAU, C. D. H. (1984). *J. Am. Chem. Soc.* **106**, 1594–1605.

BAIOCCHI, F. A., REIHER, W. & KLEMPERER, W. (1983). *J. Chem. Phys.* **79**, 6428–6429.

BARTENEV, V. N., KAMENEVA, N. G. & LIPANOV, A. A. (1987). *Acta Cryst.* B**43**, 275–280.

BROWN, I. D. (1976). *Acta Cryst.* A**32**, 24–31.

BUCKINGHAM, A. D. & FOWLER, P. W. (1983). *J. Chem. Phys.* **79**, 6426–6428.

BULANIN, M. O., BULYCHEV, V. P. & TOKHADZE, K. G. (1989). *J. Mol. Struct. (Theochem)*, **200**, 33–40.

BÜRGI, H.-B. & DUNITZ, J. D. (1988). *Acta Cryst.* B**44**, 445–448.

CAMPSTEYN, H., DUPONT, L. & DIDEBERG, O. (1974). *Acta Cryst.* B**30**, 90–94.

DAVENPORT, G. & HALL, S. (1989). *XTAL2.6 ORTEP.* Edited by S. R. HALL & J. M. STEWART. Univs. of Western Australia, Australia, and Maryland, USA.

DEL BENE, J. E. (1983). *J. Comput. Chem.* **4**, 226–233.

ETTER, M. C. (1990). *Acc. Chem. Res.* **23**, 120–126.

FRISCH, M. J., POPLE, J. A. & DEL BENE, J. E. (1985). *J. Phys. Chem.* **89**, 3664–3669.

GÖRBITZ, C. H. (1989). *Acta Cryst.* B**45**, 390–395.

GOULD, R. O., GRAY, A. M., TAYLOR, P. & WALKINSHAW, M. D. (1985). *J. Am. Chem. Soc.* **107**, 5921–5927.

HEHRE, W. J., RADOM, L., SCHLEYER, P. V. R. & POPLE, J. A. (1986). *Ab Initio Molecular Orbital Theory*, pp. 215–223. New York: Wiley–Interscience.

HURST, G. J. B., FOWLER, P. W., STONE, A. J. & BUCKINGHAM, A. D. (1986). *Int. J. Quantum Chem.* **29**, 1223–1239.

JEFFREY, G. A. & MALUSZYNSKA, H. (1990). *Acta Cryst.* B**46**, 546–549.

KOLLMAN, P. A. (1977). *Applications of Electronic Structure Theory*, edited by N. F. SCHAEFER III, ch. 3, pp. 109–152. New York, London: Plenum Press.

KROON, J., KANTERS, J. A., VAN DUIJNEVELDT-VAN DER RIJDT, J. G. C. M., VAN DUIJNEVELDT, F. B. & VLIEGENTHART, J. A. (1975). *J. Mol. Struct.* **24**, 109–129.

KRYGOWSKI, T. M. (1990). *Prog. Phys. Org. Chem.* **17**, 239–291.

LEGON, A. C. & MILLEN, D. J. (1987). *Acc. Chem. Res.* **20**, 39–46.

LESYNG, B., JEFFREY, G. A. & MALUSZYNSKA, H. (1988). *Acta Cryst.* B**44**, 193–198.

LIU, S. Y. & DYKSTRA, C. E. (1986). *J. Phys. Chem.* **90**, 3097–3103.

LLAMAS-SAIZ, A. L. & FOCES-FOCES, C. (1990). *J. Mol. Struct.* **238**, 367–382.

MALARSKI, Z., MAJERZ, I. & LIS, T. (1987). *J. Mol. Struct.* **158**, 269–377.

MITCHELL, J. B. O. & PRICE, S. L. (1989). *Chem. Phys. Lett.* **154**, 267–272.

MITCHELL, J. B. O. & PRICE, S. L. (1990). *J. Comput. Chem.* **11**, 1217–1233.

MOOTZ, D. & WUSSOW, H. G. (1981). *J. Chem. Phys.* **75**, 1517–1522.

MURRAY-RUST, P. & GLUSKER, J. P. (1984). *J. Am. Chem. Soc.* **106**, 1018–1025.

MURRAY-RUST, P. & MOTHERWELL, W. D. S. (1979). *J. Am. Chem. Soc.* **101**, 4374–4376.

PIMENTEL, G. C. & MCCLELLAN, A. D. (1960). *The Hydrogen Bond.* San Francisco: Freeman.

Precision Visuals (1987). *DI*3000. Version 5.09. Boulder, Colorado 80301, USA.

REED, A. E., WEINHOLD, F., CURTISS, L. A. & POCHATKO, D. J. (1986). *J. Chem. Phys.* **84**, 5687–5705.

SADLEJ, J. & ROOS, B. O. (1989). *Theor. Chim. Acta*, **76**, 173–185.

SCHUSTER, P., ZUNDEL, G. & SANDORFY, C. (1976). *The Hydrogen Bond – Recent Developments in Theory and Experiments*, Vols. I–III. Amsterdam: North-Holland.

SNEDECOR, G. W. & COCHRAN, W. G. (1980). *Statistical Methods*, 7th ed. Ames, Iowa: Iowa State Univ. Press.

SOMASUNDRAM, K., AMOS, R. D. & HANDY, N. C. (1986). *Theor. Chim. Acta*, **69**, 491–503.

TAFT, R. W., ABBOUD, J. L. M., KAMLET, M. J. & ABRAHAM, H. H. (1985). *J. Solution Chem.* **14**, 153–186.

TAYLOR, R. (1981). *J. Mol. Struct.* **73**, 125–136.

TAYLOR, R. & KENNARD, O. (1984). *Acc. Chem. Res.* **17**, 320–326.

TAYLOR, R., KENNARD, O. & VERSICHEL, W. (1983). *J. Am. Chem. Soc.* **105**, 5761–5766.

TAYLOR, R., KENNARD, O. & VERSICHEL, W. (1984). *Acta Cryst.* B**40**, 280–288.

VAINSHTEIN, B. K., FRIDKIN, V. M. & INDENBOM, V. L. (1982). *Modern Crystallography*, Vol. II, p. 87. Heidelberg: Springer-Verlag.

VEDANI, A. & DUNITZ, J. D. (1985). *J. Am. Chem. Soc.* **107**, 7653–7658.

WIBERG, K. B., BADER, R. F. W. & LAU, C. D. H. (1987). *J. Am. Chem. Soc.* **107**, 985–1001.